Electronic Supplementary Material (ESI) for Dalton Transactions.

Supporting Information for

A Simple Strategy for Visual Detection as well as Discrimination of Hg^{2+} and CH_3Hg^+ Species Using Fluorescent Nanoaggregates

Dr. Nilanjan Dey,[a,b,c]

[a]Graduate School of Science, Kyoto University, Sakyo, Kyoto 606-8502, Japan.

[b]Department of Chemistry, BITS-Pilani Hyderabad Campus, Shameerpet, Hyderabad-500078, Telangana, India.

Email: nilanjan@hyderabad.bits-pilani.ac.in

Experimental Section

Materials and Methods. All reagents, starting materials, and solvents were obtained from the local suppliers and used without further purification. The solvents were distilled wherever required. FT-IR spectra were recorded on a PerkinElmer FT-IR Spectrum BX system and were reported in wave numbers (cm^{-1}). ^{1}H and ^{13}C NMR spectra were recorded on a Bruker-400 Advance NMR spectrometer. Chemical shifts were reported in ppm downfield from the internal standard, tetramethylsilane. Mass spectra were recorded on a Micromass Q-TOF Micro TM spectrometer.

Sampling Procedure of Sensing. The sensing studies with metal ions was carried out by adding 10 μL DMSO solution of either **1** or **2** from a stock (1×10^{-3} M) in water to make the final volume of 1 mL ([**1**] = [**2**] = 1×10^{-5} M) followed by addition of water solution of the metal ions (1.5 equiv). In case of sensing in the buffered medium, a similar procedure has been followed for the sensing in buffered media of different pH (HCO_2Na/ HCl buffer for pH 2, Tris/HCl for pH 7 and $Na_2B_4O_7 \cdot 10H_2O$/NaOH for pH 12). In all cases, the final concentration of DMSO in the solution did not exceed 1%.

UV−Vis and Fluorescence Spectroscopy. The UV−vis and fluorescence spectroscopy were recorded on a Shimadzu model 2100 spectrometer and Cary Eclipse spectrofluorimeter respectively. The slit-width for the fluorescence experiment was kept at 5 nm (excitation) and 5 nm (emission) and the excitation wavelength was set at 320 nm for both **1** and **2**.

Fluorescence Decay Experiment. Fluorescence lifetime values were measured by using a time-correlated single photon counting fluorimeter (Horiba Jobin Yvon). The system was excited with 320 nm nano LED of Horiba - Jobin Yvon with pulse duration of 1.2 ns (slit width of 2/2, λem is 465 nm). Average fluorescence lifetimes (τ_{av}) for the exponential iterative fitting were calculated from the decay times (τ_i) and the relative amplitudes (a_i) using the following relation,

$$\tau_{av} = (a_1\tau_1^2 + a_2\tau_2^2 + a_3\tau_3^2)/(a_1\tau_1 + a_2\tau_2 + a_3\tau_3)$$

Where a_1, a_2 and a_3 are the relative amplitudes and τ_1, τ_2, and τ_3 are the lifetime values, respectively. For data fitting, a DAS6 analysis software version 6.2 was used.

Dynamic Light Scattering Studies (DLS). DLS measurements were done using a Malvern Zetasizer NanoZS particle sizer (Malvern Instruments Inc., MA) instrument. Samples were prepared and examined under dust-free conditions. Reported mean hydrodynamic diameters were obtained from Gaussian analysis of the intensity-weighted particle size distributions.

Transmission Electron Microscopy (TEM) Analysis. Transmission electron microscopy (TEM) sample was made using the drop coating method from compound 1 (10 μM) in water. TEM images were collected using a JEOL field-emission Transmission Electron Microscope (JEOL, Model JEM-2100F) under a working voltage of 80 kV.

Preparation of Paper Discs for Sensing. To prepare the compound-coated paper strips, 40 μL of $CHCl_3$-MeOH (1:1) solution of **1** (0.02 mM) was drop-cast onto the filter paper using a micropipette. The concentration of 1 in the solution as well as immersion time were optimized to obtain photostable test strips with optimal fluorescence intensity. The solution was completely absorbed in filter paper within 15 min and then the filter papers were kept overnight

to airdry. Finally, the air-dried paper strips were ready for sensing studies. The stability of paper strips was evaluated by measuring fluorescence intensity at intervals over 15 days.

Quantification studies: For quantification of Hg^{2+}, the changes in absorbance were recorded at 465 nm. The recovery values (in %) were calculated according to the following equation

%recovery = (Cadded − Ccalculated)/Cadded × 100

where Cadded is the actual concentrations of DPA spiked into the samples, and Ccalculated is their calculated values using the standard equation.

Fluorescence Quantum Yield: The fluorescence quantum yield was calculated by using rhodamine 6G (F ¼ 0.94 in EtOH) as a reference. And the quantum yield is calculated using the equation,

$$\Phi_{unk} = \Phi_{std} [(I_{unk}/A_{unk})/(I_{std}/A_{std})](\eta_{unk}/\eta_{std})^2$$

where, Φ_{unk} and Φ_{std} are the radiative quantum yields of the sample and standard, I_{unk} and I_{std} are the integrated emission intensities of the corrected spectra for the sample and standard, A_{unk} and A_{std} are the absorbances of the sample and standard at the excitation wavelength, and η_{unk} and η_{std} are the indices of refraction of the sample and standard solutions, respectively

Analysis of Real-Life Samples. To evaluate the efficiency of **1** in estimating Hg^{2+} in environmental samples, the performance of the present method was examined by testing tap water, pond water, and seawater samples. The tap water samples were collected from the laboratory. The pond water samples were collected from local pond at Kolkata, West Bengal, India. The seawater samples were collected from the Arabian Sea (near Mangalore beach). The tap water and pond water samples were subjected to analysis as received. However, the seawater samples were filtered through a 0.22 μm membrane to remove the insoluble dirt particles. The water samples were spiked with different amounts of Hg^{2+} more than 2 h before the analysis.

Cell Culture. HeLa cells were cultured in Dulbecco's Modified Eagle's Medium (DMEM, CELL clone, India) containing 10% FBS (Invitrogen, USA) and antibiotics (100 units/mL penicillin and 100 μg/mL streptomycin). Cells were incubated in a humidified 5% CO_2 incubator (Sanyo, UK) at 37 °C.

Cell Viability Assay. Cytotoxicity of the compound **1** was evaluated in HeLa cells by the 3-(4,5-dimethylthiazol-2-yl)-2,5- diphenyltetrazolium bromide (MTT) assay. In a typical experiment, cells were seeded at a density of $\sim 1 \times 10^4$ cells/ well in the 96 well plates and incubated for 24 h. Then, the cells were treated with different concentrations of the probe (0 – 50 μM). Finally, cells were washed, and 20 μL of MTT (5 mg/mL in DMEM) was added in each well and incubated for 3 h in the dark. Finally, whole medium was removed from the wells, and DMSO (100 μL) was added. The cells were incubated for 5 min in the dark, and absorbance was measured at 560 nm.

Cell Imaging. For the blank reading, the cells were incubated with 10 μM of compound **1** for 40 min at 37 °C. Then, the medium was removed, and the cells were washed multiple times with pH 7.4 DMEM buffer. To check the mercury induced emission quenching, the cells were incubated with 20 mM of Hg^{2+} and CH_3Hg^+ for 2 h, followed by treatment with compound **1**

for 40 min. Finally, the florescence images were obtained with and without the presence of Hg^{2+} and CH_3Hg^+ using fluorescence microscopy.

Synthesis of Compound 1 and 2

The compound **1** was synthesized following the literature reported procedure.

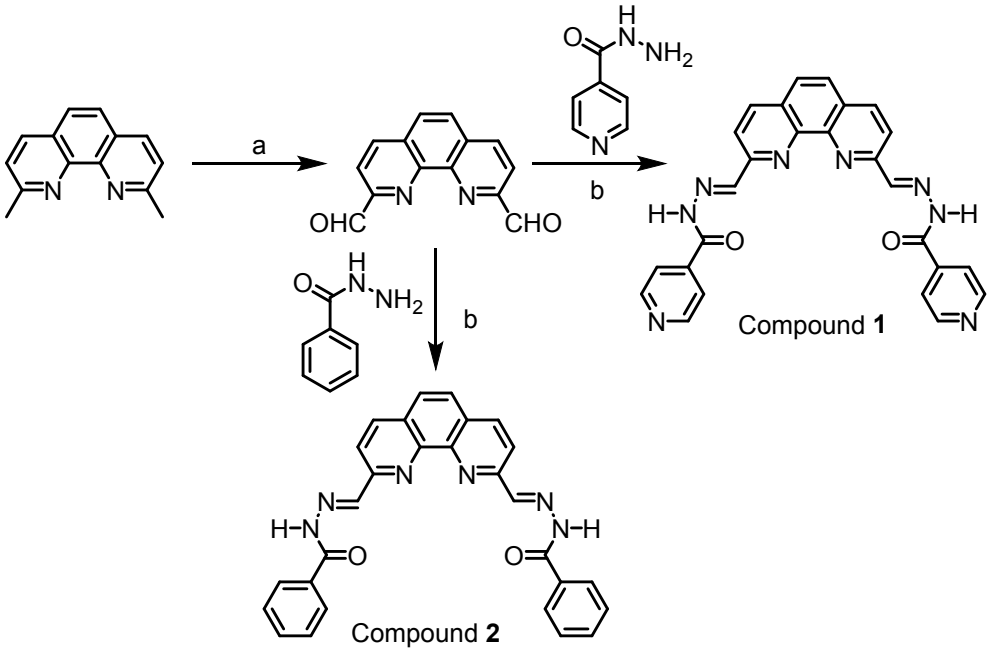

Scheme 1. (a) SeO_2, dioxane/water (95:5 v/v) reflux, 2 h, 45%; (b) MeOH, reflux, 6 h, 82 % (for **1**) and 75 % (for **2**).

Additional Spectral Data

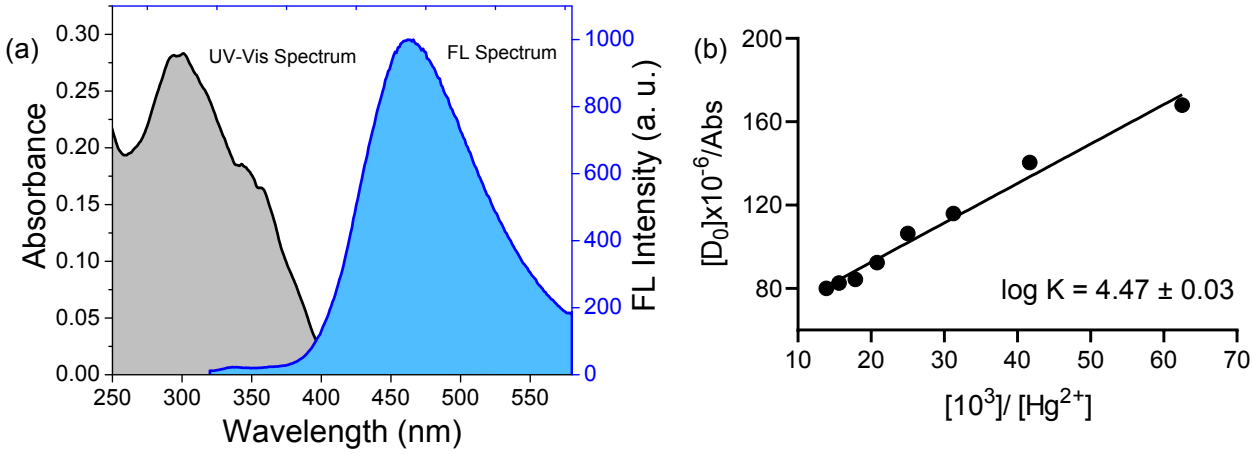

Figure S1. (a) UV-visible and fluorescence spectra of **1** (10 μM, λex: 320 nm) at pH 7.0 in PBS Buffer. (b) Binding constant of **1** with Hg^{2+} considering 1:1 binding model, $[D_0]$ = concentration of **1** = 10 μM.

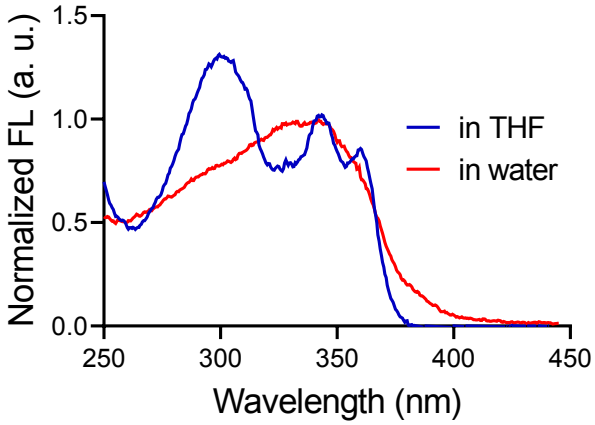

Figure S2. Fluorescence excitation spectra of **1** (10 μM, λem: 454 nm) in THF and water medium (at pH 7.0 in PBS Buffer).

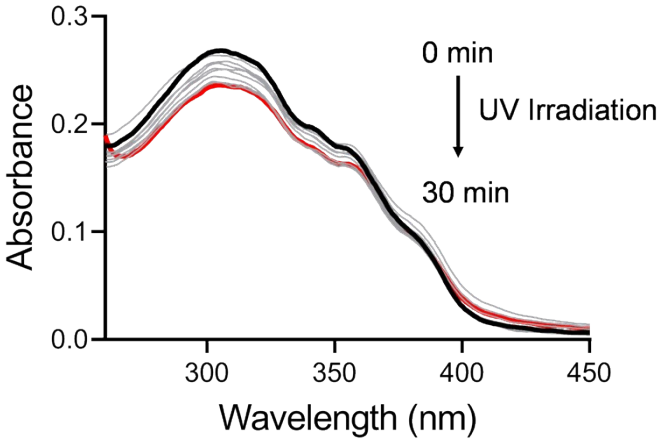

Figure S3. UV-visible spectra of **1** (10 μM) upon irradiation with UV light (300 mW cm^{-2}) for 30 min.

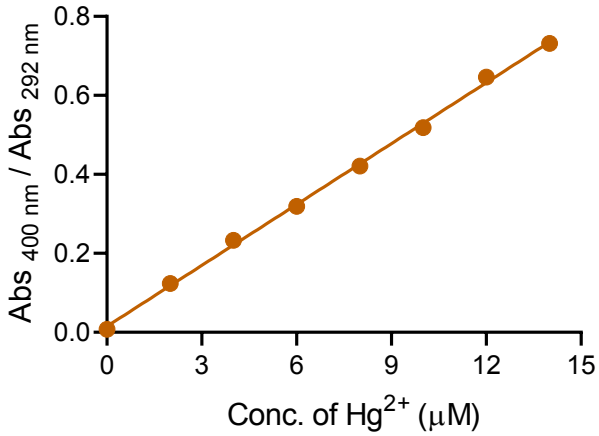

Figure S4. Changes in absorbance of **1** (10 μM) with Hg^{2+} ion at pH 7.0 in PBS Buffer (ratiometric response).

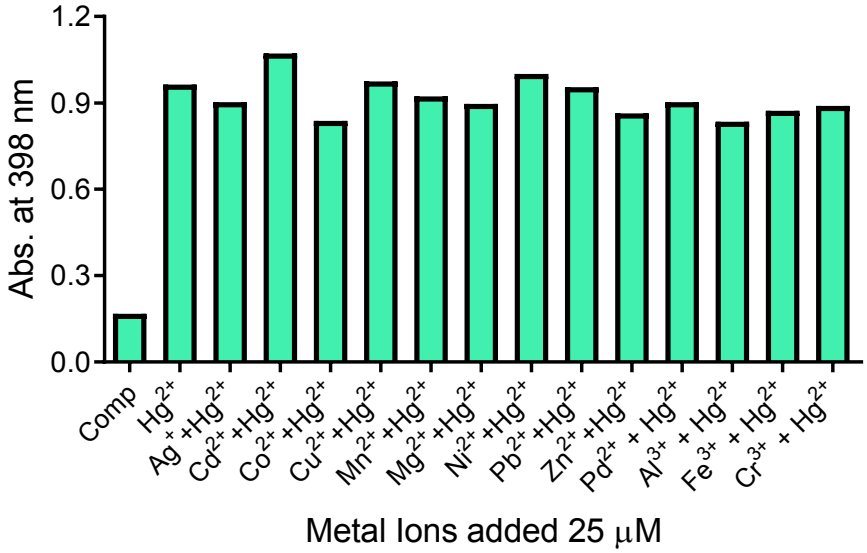

Figure S5. Change in absorbance of **1** (10 μM) upon addition of Hg^{2+} (15 μM) in presence of other competing metal ions (25 μM).

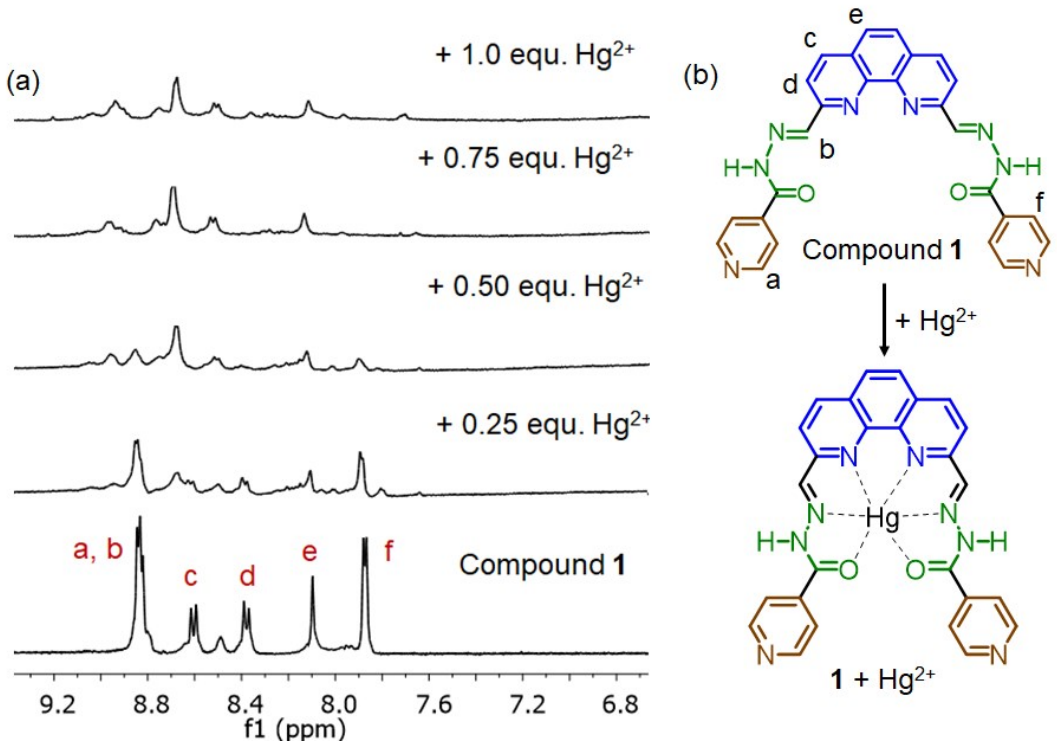

Figure S6. (a) Partial ^{1}H-NMR spectra of **1** (5 mM) upon addition of Hg^{2+} (0 – 1 equiv.) in DMSO-d_6/ D_2O (1:1) mixture medium. (b) Interaction of **1** with Hg^{2+} (the relevant protons have been shown in the structure).

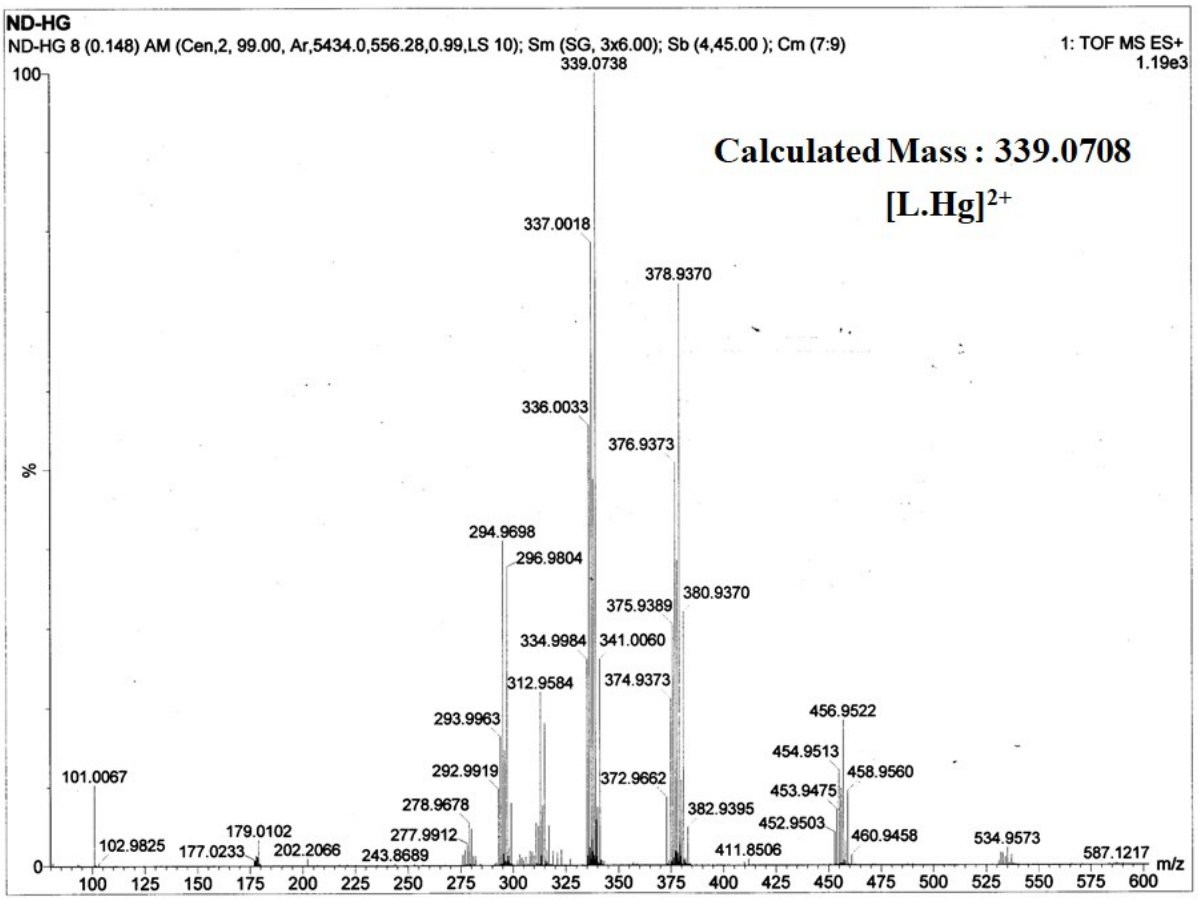

Figure S7. ESI-MS mass spectrum of **1** + Hg^{2+} indicates 1:1 complex formation.

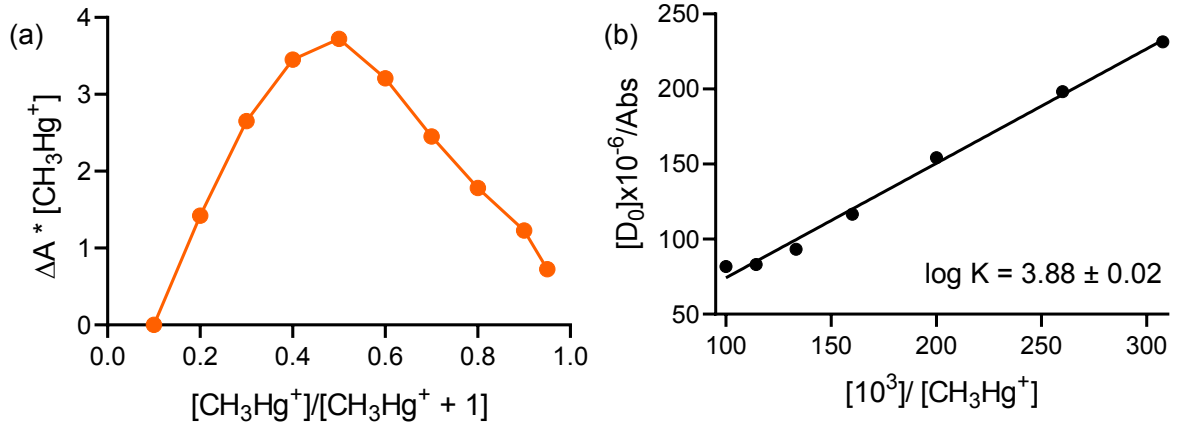

Figure S8. (a) Job's plot analysis of **1** with CH_3Hg^+ at pH 7.0 in PBS Buffer. (b) Binding constant of **1** with CH_3Hg^+ using Benesi-Hildebrand method for 1:1 model.

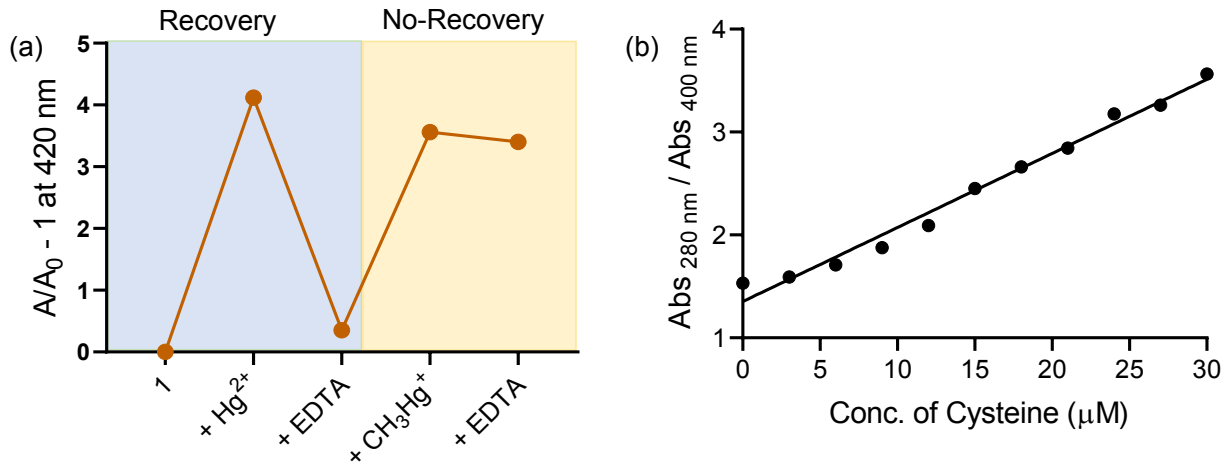

Figure S9. (a) Reversibility checking of **1** with Hg^{2+} and CH_3Hg^+ by EDTA at pH 7.0 in PBS Buffer. (b) Change in absorbance of **1** + Hg^{2+} (10 μM, 1:1) upon addition of cysteine at pH 7.0 in PBS Buffer.

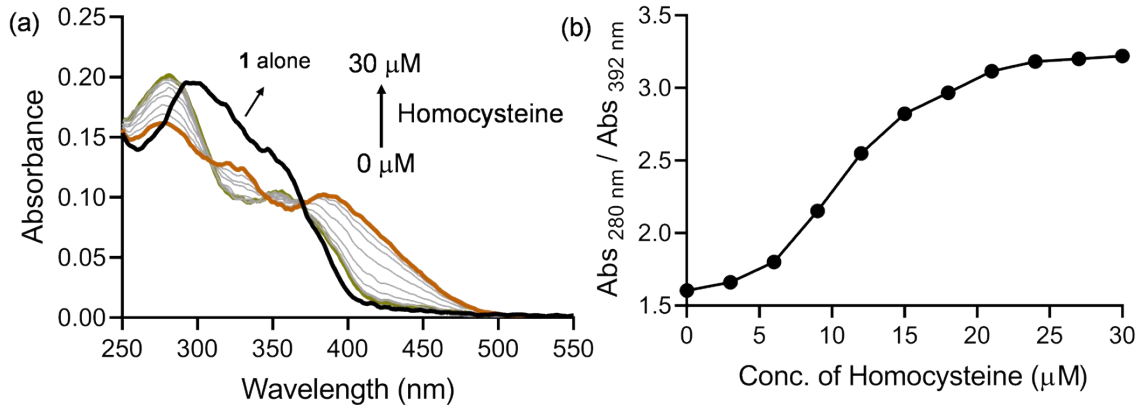

Figure S10. (a) UV-visible titration of **1** + Hg^{2+} (10 μM, 1:1) with homocysteine at pH 7.0 in PBS buffer. (b) Change in absorbance of **1** + Hg^{2+} (10 μM, 1:1) upon addition of homocysteine at pH 7.0 in PBS Buffer.

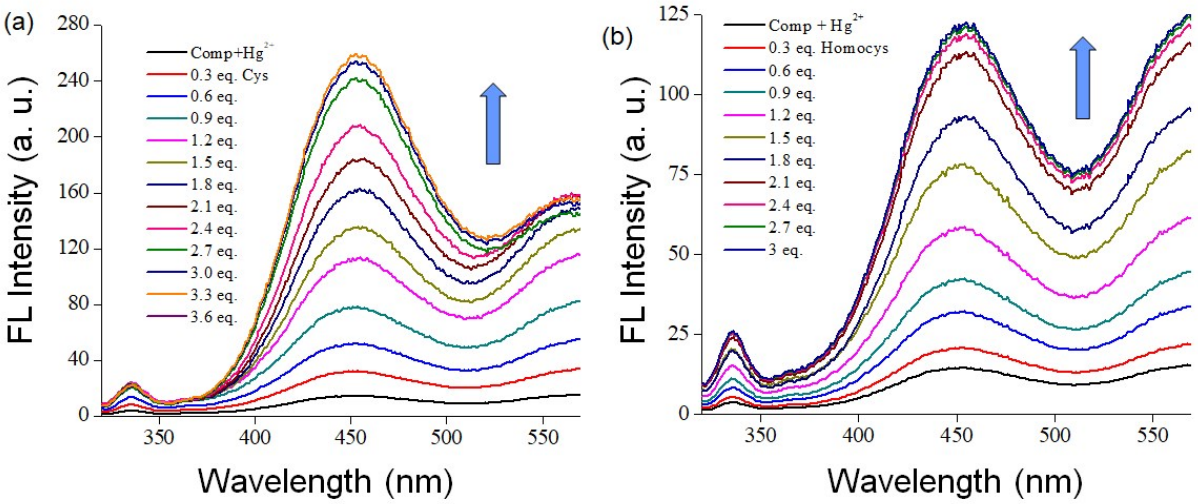

Figure S11. (a) Fluorescence spectra of **1** + Hg^{2+} (10 μM, 1:1) by λex: 320 nm with cysteine at pH 7.0 in PBS Buffer. (b) Fluorescence spectra of **1** + Hg^{2+} (10 μM, 1:1) by λex: 320 nm with homocysteine at pH 7.0 in PBS Buffer.

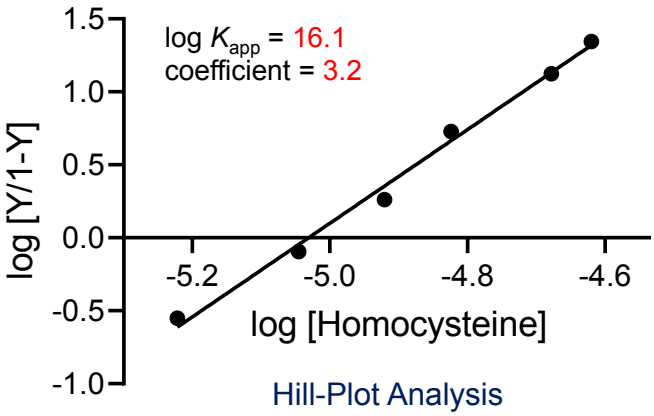

Figure S12. Hill-plot analysis shows 'cooperative binding' of homocysteine with **1** + Hg^{2+} (10 μM, 1:1) at pH 7.0 in PBS buffer.

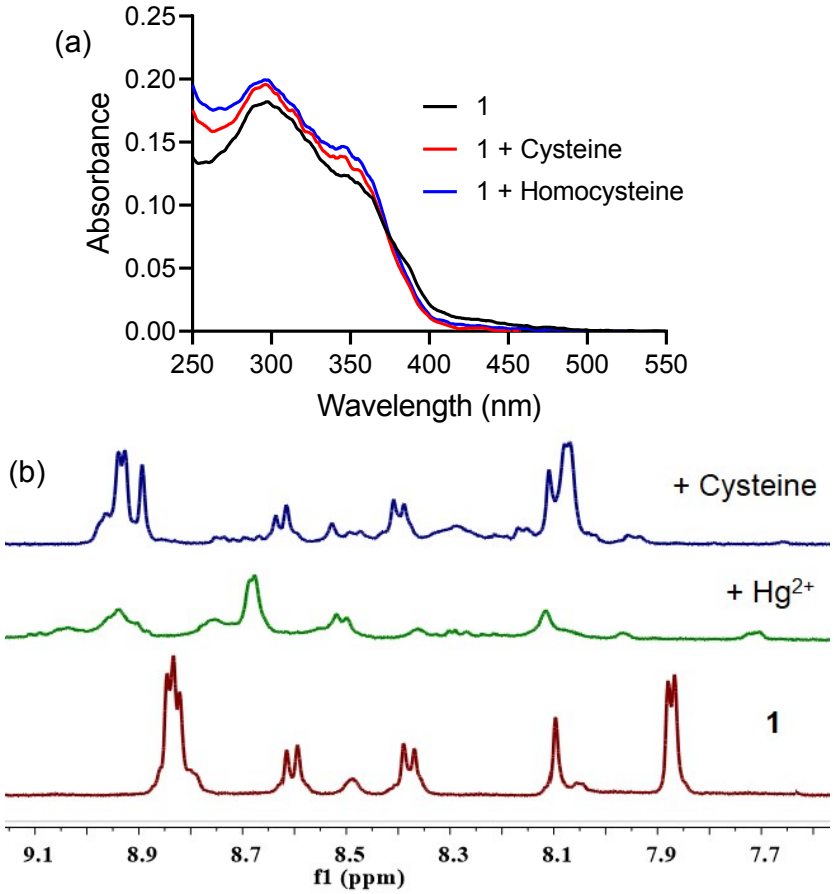

Figure S13. (a) UV-visible spectra of **1** (10 μM) with cysteine and homocysteine at pH 7.0 in PBS buffer. (b) Partial ^{1}H-NMR spectra of **1** (5 mM) upon addition of Hg^{2+} (1 equiv.) and cysteine (3 equiv.) in DMSO-d_6/ D_2O (1:1) mixture medium.

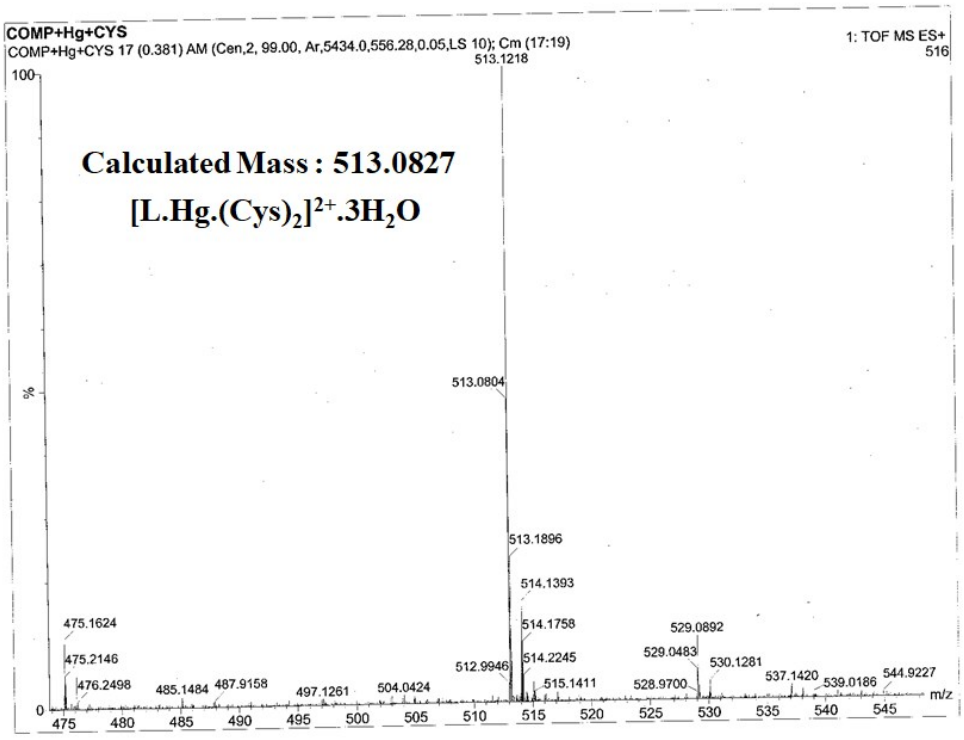

Figure S14. ESI-MS mass spectrum of **1** + Hg^{2+} with cysteine indicates 1:1:2 complex formation.

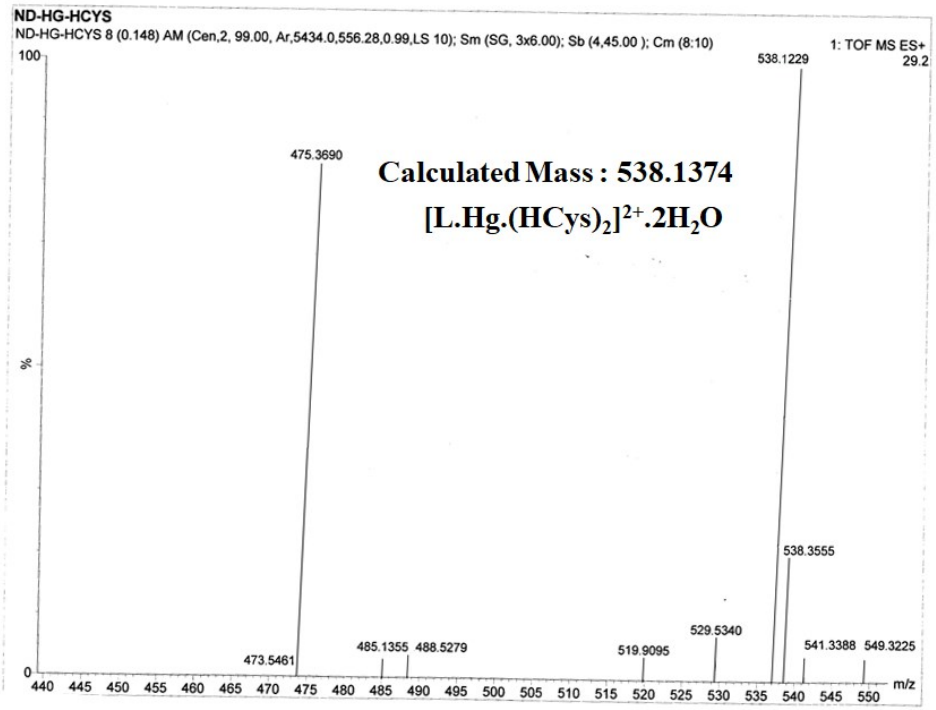

Figure S15. ESI-MS mass spectrum of **1** + Hg^{2+} with homocysteine indicates 1:1:2 complex formation.

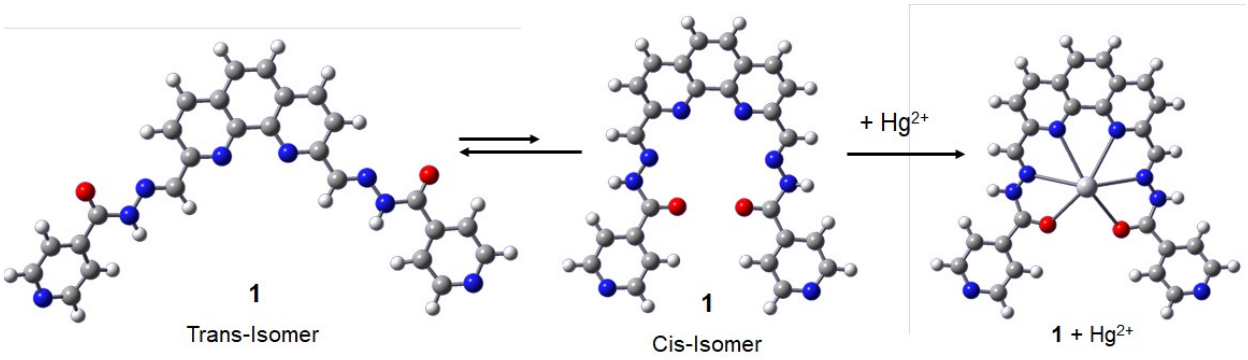

Figure S16. Energy minimized structures of **1** (cis and trans isomers) and corresponding Hg^{2+} complex using B3LYP level of theory with 6-31G* basis set for C, H, N, O and LANL2DZ for Hg.

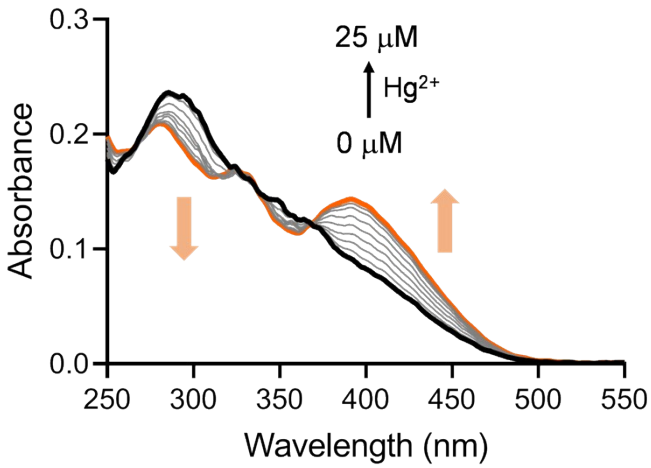

Figure S17. UV-visible titration of **1** (10 μM) with Hg^{2+} (0 – 25 μM) at pH 7.0 in PBS buffer (with ~0.1 mg/mL HSA).

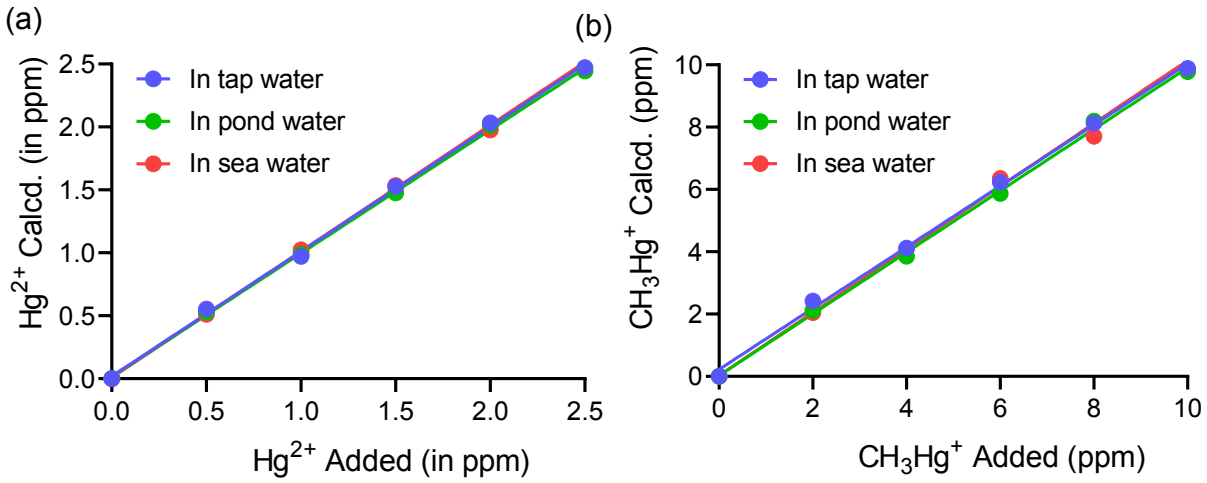

Figure S18. (a) Change in absorbance of **1** (10 μM) upon addition of Hg^{2+} (0- 2.5 ppm) in different water samples (at pH 7.0) [Recovery plot]. (b) Change in absorbance of **1** (10 μM) upon addition of CH_3Hg^+ (0- 10 ppm) in different water samples (at pH 7.0) [Recovery plot].

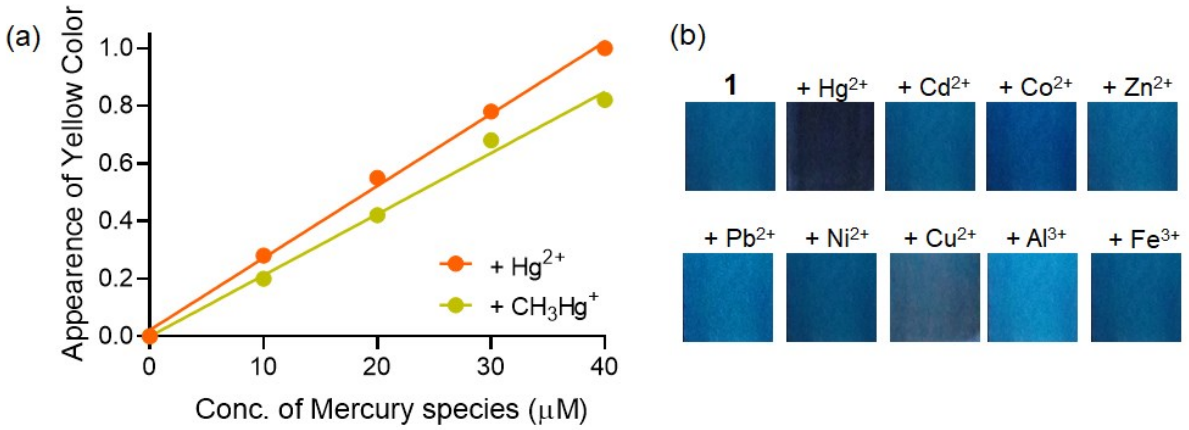

Figure S19. (a) Changes in color intensity of test strips (paper strips coated with **1**) upon addition of Hg^{2+}, quantified by ImageJ software. (b) Change in fluorescence color of test strips (paper strips coated with **1**) upon of different metal ions.

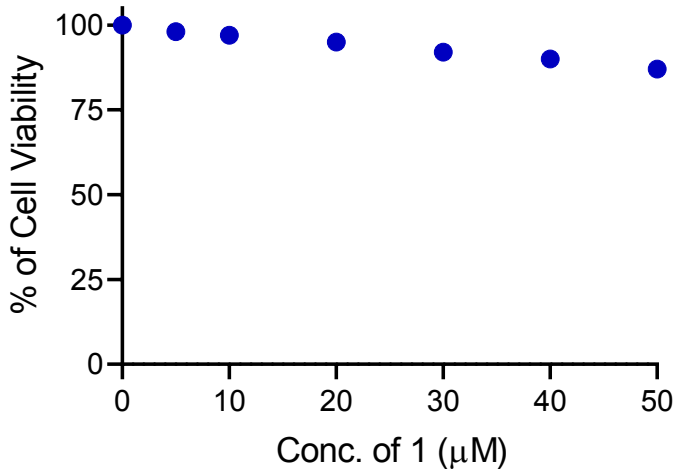

Figure S20. Cell-viability assay of HeLa cells in presence of compound **1** (using MTT as indicator dye).

System	Detection mode	Medium	Detection limit	Time	Application	Reference
Europium Cluster	Luminescence (interference from Zn^{2+}, Fe^{3+}, Cd^{2+}, Ag^{+})	water	0.8 μg L^{-1}	24 h	Analysis of natural water samples	Sens Actuators B: Chem, 2017, 248, 589-596
Coumarin-based dye	Fluorescence (same response with Hg^{2+} and CH_3Hg^{+})	PBS buffer (pH 7.4)	Hg^{2+} (27 nM) CH_3Hg^{+} (5.8 μM)	30 min (for CH_3Hg^{+}), 4 min (for Hg^{2+})	imaging in both cells and Escherichia coli	Chem. Commun., 2018, 54, 4955-4958
TPE−monoboronic acid	Fluorescence (same response with Hg^{2+} and CH_3Hg^{+})	water−THF mixture (9:1 v/v)	Hg^{2+} (0.12 ppm)	30 min	Imaging in Zebra fish	Anal. Chem. 2017, 89, 12698−12704
Dansyl−monoboronic acid	Fluorescence (same response with Hg^{2+} and CH_3Hg^{+})	Water (1% CH_3CN)	Hg^{2+} (4 nM) CH_3Hg^{+} (200 ppb)	5 min (for CH_3Hg^{+}), 2 min (for Hg^{2+})	Cell imaging	Chem. Commun., 2020, 56, 2941-2944
Spirooxazine derivative	Color change (same response with Hg^{2+} and CH_3Hg^{+})	Dioxane	Hg^{2+} (152 nM) CH_3Hg^{+} (150 nM)	~20 sec	Paper strips	Dyes Pigm, 2021, 186, 108996.
Rhodamine based dye	Fluorescence change (same response with Hg^{2+} and CH_3Hg+)	Water (1% DMSO)	CH_3Hg^{+} (200 nM)	5 min	Cell imaging	Org. Biomol. Chem., 2009, 7, 4590–4593
Dansyl based dye	Fluorescence change (discrimination between Hg^{2+} and CH_3Hg^{+})	SDS micelle	Hg^{2+} (1.8 ppb) CH_3Hg^{+} (44.4 ppb)	30 min (for CH_3Hg^{+})	Cell imaging	Anal. Chem. 2020, 92, 4917−4925
Phenanthroline-based dye	Color change (discrimination between Hg^{2+} and CH_3Hg^{+})	PBS buffer (pH 7.4)	Hg^{2+} (4.8 ppb) CH_3Hg^{+} (18.2 ppb)	10 min (for CH_3Hg^{+})	Analysis of natural water samples, Paper strips, cell imaging	In this work*

Table S1. A comparison with published reports on simultaneous sensing of Hg^{2+} and CH_3Hg^{+}.